Solvent Dynamical Behavior in an Organogel Phase As Studied by NMR Relaxation and Diffusion Experiments

ARTICLE *in* THE JOURNAL OF PHYSICAL CHEMISTRY B · FEBRUARY 2011

Impact Factor: 3.3 · DOI: 10.1021/jp200281f · Source: PubMed

THE JOURNAL OF PHYSICAL CHEMISTRY B

ARTICLE

pubs.acs.org/JPCB

Solvent Dynamical Behavior in an Organogel Phase As Studied by NMR Relaxation and Diffusion Experiments

Mehdi Yemloul,[†] Emilie Steiner,[†] Anthony Robert,[†] Sabine Bouguet-Bonnet,[†] Florent Allix,[‡] Brigitte Jamart-Grégoire,[‡] and Daniel Canet*[,†]

[†]Méthodologie RMN, CRM[2] (UMR 7036, UHP-CNRS), Faculté des Sciences et Techniques, B.P. 239, 54506 Vandœuvre-lès-Nancy (Cedex), France

[‡]Laboratoire de Chimie Physique Macromoléculaire, LCPM (UMR 7568, INPL-CNRS), 1 Rue Grandville, B.P. 451, 54001 Nancy (Cedex), France

ABSTRACT: An organogelation process depends on the gelator−solvent pair. This study deals with the solvent dynamics once the gelation process is completed. The first approach used is relaxometry, i.e., the measurement of toluene proton longitudinal relaxation time T_1 as a function of the proton NMR resonance frequency (here in the 5kHz to 400 MHz range). Pure toluene exhibits an unexpected T_1 variation, which has been identified as paramagnetic relaxation resulting from an interaction of toluene with dissolved oxygen. In the gel phase, this contribution is retrieved with, in addition, a strong decay at low frequencies assigned to toluene molecules within the gel fibers. Comparison of dispersion curves of pure toluene and toluene in the gel phase leads to an estimate of the proportion of toluene embedded within the organogel (found around 40%). The second approach is based on carbon-13 T_1 and nuclear Overhauser effect measurements, the combination of these two parameters providing direct information about the reorientation of C−H bonds. It appears clearly that reorientation of toluene is the same in pure liquid and in the gel phase. The only noticeable changes in carbon-13 longitudinal relaxation times are due to the so-called chemical shift anisotropy (csa) mechanism and reflect slight modifications of the toluene electronic distribution in the gel phase. NMR diffusion measurements by the pulse gradient spin-echo (PGSE) method allow us to determine the diffusion coefficient of toluene inside the organogel. It is roughly two-thirds of the one in pure toluene, thus indicating that self-diffusion is the only dynamical parameter to be slightly affected when the solvent is inside the gel structure. The whole set of experimental observations leads to the conclusion that, once the gel is formed, the solvent becomes essentially passive, although an important fraction is located within the gel structure.

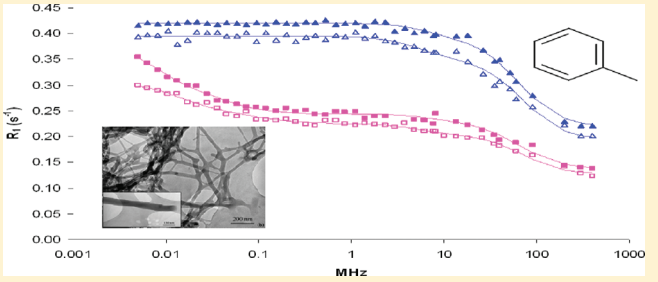

INTRODUCTION

Organogels are generally formed by a self-aggregation of gelators, leading to the formation of fibrous three-dimentional networks with cross-links among the nanofibers possibly entrapping the solvent.[1−8]

Due to present and potential applications, organogels have attracted much interest. Various molecules are prone to form an organogel in an appropriate solvent, and, recently, a new class of strong low-molecular-weight organogelators, based on amino-acid derivatives, has come out.[9,10] In the fibers, gelator molecules are assembled through gelator−gelator interactions involving noncovalent bonding[1,11] (H-bonding, van der Waals, π-stacking, etc.) with a strong self-complementarity and unidirectional intermolecular cohesion. Indeed, gelator−solvent interactions[12] sometimes seem to influence the molecular arrangement, the morphology of the fibers and the junction zones. It is well established that the choice of the pair organogelator−solvent has a major importance in the search for specific properties of the material. However, if much attention has been paid to gelators, the solvent is usually chosen by a trial-and-error approach. The problem that we address here is the fate of the solvent (through its dynamical properties) once the gelation process is over. This is an important issue as far as material properties are concerned. This issue is related to the presence or absence of the solvent within the fibril bundles and, more generally, to possible interactions between gel and solvent. Indeed, for interpreting results from circular dichroism (CD) and small-angle X-ray scattering (SAXS), Jeong et al.[12] postulate the existence of wet and dry organogels according to the presence or absence of the solvent within the fiber network.

In this work, we have studied an organogel formed in toluene with the gelator schematized in Figure 1. The first set of experiments was the measurement of the longitudinal relaxation time T_1 of toluene protons in a very broad frequency range (5 kHz to 400 MHz) by means of instruments operating at different values of the static magnetic field B_0 (since the resonance frequency is directly proportional to B_0). This method, called

Received: January 11, 2011
Revised: February 3, 2011
Published: February 28, 2011

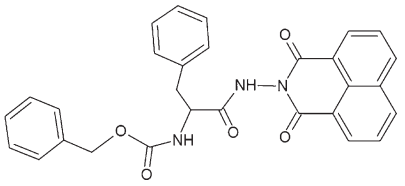

Figure 1. Chemical structure of the gelator used in the present study.

"relaxometry", is in principle very sensitive to slow motions and thus well suited for determining the proportion of molecules in fast exchange between, say, a surface and the bulk. Here the method unambiguously revealed the presence of toluene within the organogel, which can therefore be classified as wet.[12] Proton relaxometry experiments were complemented by carbon-13 T_1 and nuclear Overhauser effect (NOE) measurements performed again at different frequencies. Their interest lies in the fact they exclusively probe the reorientational dynamics through intramolecular interactions, while proton T_1 depends on both inter- and intramolecular interactions. Some additional deuterium T_1 measurements have been performed just to confirm the conclusions derived from carbon-13 relaxation. Finally, translational motions were investigated by NMR measurements of toluene self-diffusion coefficients. All these measurements should be amenable to provide a realistic dynamical picture (rotation *and* translation) of the solvent in a organogel phase and to determine whether it plays any role in the gel structure or duration.

EXPERIMENTAL SECTION

The organogelator was synthesized according to procedures described previously.[10] It was dissolved in toluene at 0.5 wt %. Toluene was of commercial provenance (VWR, France) and used without further purification. Because sensitivity of the NMR experiments at low frequencies is a problem that can be alleviated by larger samples, sealed 10 mm o.d. NMR sample tubes (rather than standard 5 mm o.d. tubes) were prepared. These samples were also used at high frequencies (for which sensitivity is no longer a problem) in order to avoid any systematic error that could arise from slight concentration variations (if other samples were used).

Several instruments were employed for ^{1}H NMR relaxometry experiments: a SMARTracer relaxometer (Stelar Company, Mede, Italy) for the 5 kHz-10 MHz frequency range; a homemade spectrometer equipped with a variable field electromagnet for the 8 MHz to 90 MHz range; a homemade spectrometer operating at 200 MHz; and two Bruker Avance spectrometers operating at 300 and 400 MHz. Experiments performed with the relaxometer are run at low resolution according to the fast field cycling procedure.[13] As a consequence, it is the global (of all protons) longitudinal relaxation time which is measured. It must be noticed that, at these low values of the magnetic field and owing to the inhomogeneity of the latter, the two toluene resonances totally overlap, and the measured relaxation rate (R_1, which is the inverse of the relaxation time T_1) is actually a linear combination of the aromatic and methyl relaxation rates:

$$R_1^{\text{measured}} = \frac{3}{8} R_1^{\text{methyl}} + \frac{5}{8} R_1^{\text{aromatic}} \qquad (1)$$

With the other instruments, the aromatic and methyl resonances are resolved, and their relaxation times are measured *separately*. For being comparable to the relaxometer data, global relaxation rates must be calculated from experimental data according to eq 1 so as to continue the first part of the dispersion curve. At 200, 300, and 400 MHz, relaxation times were measured by the usual inversion−recovery method. Due to some instability of the variable field magnet, measurements between 8 and 90 MHz had to be performed swiftly. We had recourse to a procedure developed previously,[14] which is based on the acquisition of only two data points: one close to the initial perturbation (for example, an inverting or a saturating pulse), the other around the expected T_1, in addition to a separate measurement aimed at determining the equilibrium value (requiring repetition intervals of the order of $5T_1$). In some instances, when the inverting pulse was of poor quality, it was simply replaced by a 90° pulse which, because of short effective transverse relaxation times, plays the same role as a saturating pulse. For all the instruments, the sample temperature was carefully controlled since relaxation times may be temperature dependent. In such a situation, the frequency variation of T_1 could be masked by effects arising from slight temperature fluctuations.

Carbon-13 longitudinal relaxation times and NOE factors were measured with three Avance Bruker NMR spectrometers operating respectively at the carbon-13 resonance frequencies of 75, 100, and 150 MHz and with the 10 mm o.d. sample tubes used for the proton relaxometry measurements. Only the carbons (C_2, C_3, C_4) directly bound to a proton were considered. As carbon-13 relaxation times of toluene are long, the saturation-recovery method was preferred because it avoids the long waiting time of the inversion-recovery method. Raw data are fitted against $A(1 - Ke^{-t/T1})$, where A is a scaling factor, while K accounts for any saturation imperfection (ideally it would be equal to 1; in practice it can be higher or smaller than 1). For T_1 measurements, proton decoupling was applied continuously. NOE measurements require two distinct experiments that differ by the state of proton magnetization. Let us call I_{stat} a peak intensity measured under continuous proton decoupling (as proton magnetization is saturated, a new steady state is reached for carbon-13 magnetization) and I_0 the intensity measured when decoupling is on only during data acquisition (proton magnetization is at equilibrium prior the measurement of carbon-13 magnetization, which is therefore also at thermal equilibrium). The NOE factor η is given by $\eta = (I_{\text{stat}} - I_0)/I_0$.

The other experiments (including deuterium relaxation and diffusion measurements) were performed with deuterated toluene in 5 mm o.d. tubes. Deuterium longitudinal relaxation times were measured with toluene-d_5 at 13.6 MHz with the variable field spectrometer and at 30.55 MHz, 46.07 and 61.1 MHz with the Bruker spectrometers mentioned above. Self-diffusion coefficients were measured from the residual protons of perdeuterated toluene with the 400 MHz spectrometer using the standard stimulated echo method with bipolar gradient pulses.

TOLUENE PROTON RELAXOMETRY

Results. Two series of experiments have been carried out: one at 20 °C, the other at 30 °C, these temperatures corresponding unambiguously to the gel phase for the sample containing the gelator. The other sample investigated was that of pure toluene. Full dispersion curves, for both samples and at both

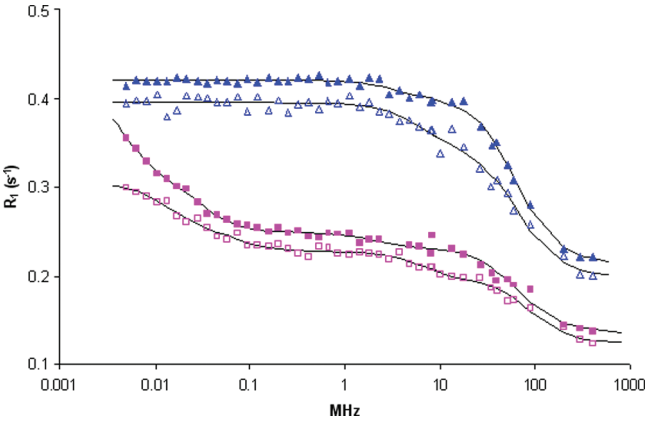

Figure 2. Dispersion curves for pure toluene (top) and toluene with the gelator (gel phase, bottom). Filled symbols: 20 °C; open symbols: 30 °C. Solid curves: recalculated with the parameters deduced from the best fit of experimental data.

temperatures, are shown in Figure 2. They represent the graphical variation of $3/8R_1^{\text{methyl}} + 5/8R_1^{\text{aromatic}}$.

Dispersion curves of pure toluene are perfect Lorentzian curves that would occur for usual relaxation mechanisms (for instance proton−proton dipolar interaction) in the case of slow molecular motions (characterized by a large correlation time) originating from a large molecular size or from a highly viscous medium. Of course, these conditions are not met here because toluene is a nonviscous liquid and, as a consequence, correlation times (τ_c) have to be around 10^{-11}−10^{-12} s. In fact, it is not τ_c alone that matters, but rather the product $\omega\tau_c$, where ω is a resonance frequency (see below). In the case of proton−proton dipolar interaction, ω would be the proton resonance frequency (or twice this frequency) and would not be large enough for producing a Lorentzian dispersion curve. However, if we envision dipolar interactions with the unpaired electron of the oxygen molecule, we must consider the electron resonance frequency, which is 658 times larger than the proton resonance frequency. This feature explains these unexpected dispersion curves, an explanation that is confirmed by a degassed sample (not shown). As a matter of fact, similar dispersion curves have been obtained for a series of solvents equilibrated with oxygen[15] and corroborate our observations. The particular dispersion curve of pure toluene is still visible in the dispersion curve of the sample with the gelator (see Figure 2). However, it represents roughly half of the curve with the superposition of a fast decay at low frequencies (smaller than 100 kHz). This decay is undoubtedly the fingerprint of specific interactions experienced by toluene molecules in the presence of a somehow rigid structure, namely, the gel fibers.

Analysis of Dispersion Curves. The dispersion curve of pure toluene stems from paramagnetic relaxation, which is due to the dipolar interaction of an unpaired electron (in the dioxygen molecule) with the nuclear spins. Its contribution to the relaxation rate can be written as[16,17]

$$R_1^{\text{para}} = K_{\text{para}}[7\tilde{J}(\omega_e) + 3\tilde{J}(\omega_H)] \quad (2)$$

where K_{para} includes various constants and $1/r_{eH}^6$ (r_{eH} being the distance between the unpaired electron and the considered proton). $\mathcal{J}(\omega)$ is a normalized spectral density, its simplest form being

$$\tilde{J}(\omega) = \frac{2\tau_c}{1+\omega^2\tau_c^2} \quad (3)$$

Table 1. Results Derived from ^{1}H Dispersion Curves of Pure Toluene at the Two Measurement Temperatures

	20 °C	30 °C
A (s^{-1})	0.127 ± 0.003	0.118 ± 0.003
$\tau_{c,arom}$ (ps)	68 ± 12	39 ± 8
b_{arom} (s^{-2})	(1.4 ± 1) 10^8	(6 ± 4) 10^8
τ_{c,CH_3} (ps)	3.9 ± 0.2	3.6 ± 0.4
b_{CH_3} (s^{-2})	(12.6 ± 0.6) 10^{10}	(10.5 ± 1.0) 10^{10}

where τ_c is an effective correlation time including,[18] among other things, the correlation time associated with the motion of the r_{eH} vector. To a first approximation, it can be assumed that this latter contribution is predominant. This would imply that it is reorientational by nature, the distance between the toluene molecule and the dioxygen molecule being quasi-constant as it can be inferred from the likely affinity of oxygen for toluene. In eq 2, $\omega_e = 658\omega_H$ and ω_H are respectively the electron and proton resonance frequencies (in rad·s^{-1}). Because toluene is a small molecule, τ_c is very short so that $\mathcal{J}(\omega_H)$ is frequency independent (extreme narrowing conditions). These latter conditions apply as well to other relaxation mechanisms (for instance proton−proton dipolar interactions) and, referring to eqs 1 and 2, the global relaxation rate for toluene in the liquid phase can be written as

$$R_1(\omega_H) = A + \frac{5}{8}\frac{b_{arom}(2\tau_{c,arom})}{1+(658\omega_H\tau_{c,\,arom})^2} + \frac{3}{8}\frac{b_{CH3}(2\tau_{c,CH3})}{1+(658\omega_H\tau_{c,CH3})^2} \quad (4)$$

A contains all frequency independent contributions, namely $\mathcal{J}(\omega_H)$ of the paramagnetic contribution in addition to the other proton−proton dipolar contributions. The b parameters are related to the electron−proton dipolar interactions and are by essence structural quantities. Results of the fit to experimental data (the numerical procedures will be described in a separate publication) are reported in Table 1 and shown graphically in Figure 2. The only parameters of interest are correlation times. They cannot be exactly those of the literature[19] because the latter are deduced from intramolecular dipolar interactions, modulated by molecular reorientation. By contrast, our correlation times reflect the modulation of an intermolecular dipolar interaction (between the oxygen unpaired electron and the toluene protons). Again, due to the order of magnitude of correlation times, this modulation should be essentially of reorientational nature. However, the correlation time deduced from the aromatic proton data is probably unrealistic due to the low weight of the corresponding contribution (see the b parameters). Conversely, the correlation time (4 ps) deduced from the methyl proton data (which constitute a predominant contribution) is in agreement with literature findings.[15] On the other hand, these correlation times are, as expected, temperature dependent, being smaller at 30 °C than at 20 °C.

Turning now to the dispersion curve of toluene in the gel phase, we have to consider that the observed relaxation rate R_1 can be expressed as

$$R_1^{\text{obs}} = pR_1^{\text{in}} + (1-p)R_1^{\text{out}} \quad (5)$$

where p is the proportion of toluene molecules embedded within the gel structure thus possessing a specific relaxation rate R_1^{in}, R_1^{out} being expected to be close to the relaxation rate of pure toluene. A global fit has been successfully performed, the whole set of

results is not reported because these parameters are not really relevant to the problem addressed in the present study (at the exception of the correlation times characterizing the fast initial decay and which will simply be alluded to when necessary). We shall just mention that attempts to ascribe the fast low frequency decay to paramagnetic relaxation failed because the effect of the other spectral density, $3J(\omega_H)$, implied in eq 2 could not be detected in the experimental dispersion curves. Consequently, this fast initial decay can be attributed either to a reorientational process strongly hindered by the gel surface or to intermolecular dipolar interactions with the spins of the gel surface, both phenomena being anyway mediated by translational diffusion. These points will be further discussed later and it will be shown that a reorientational process cannot be invoked. Indeed, spectral densities, in the case of intermolecular dipolar interactions, are known to be frequency dependent[20] and could reach large values at very low frequencies.[21] Nevertheless, the merit of this dispersion curve analysis is to clearly characterize and identify the different relaxation regimes, noticeably to bring out the presence of solvent within the gel structure (see figure 3 for a low-frequency expansion of the dispersion curves). As a matter of fact, comparing the plateau values for pure toluene and toluene in the gel phase should lead to a reasonable estimate of p if it is assumed that the gel phase value can be identified with the pure toluene value multiplied by $(1\text{-}p)$. We find $p \approx 0.4$ at both temperatures (20 and 30 °C). We shall retain this result, although it rests on the assumption that "out" toluene behaves similarly as pure toluene. In fact, this assumption is not unreasonable in view of the conclusions of the forthcoming section.

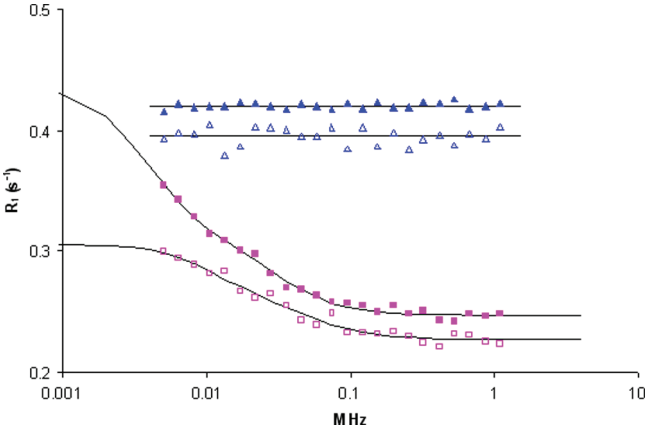

Figure 3. Low frequency parts of the dispersion curves of pure toluene (top) and toluene with the gelator (gel phase, bottom). Filled symbols: 20 °C; empty symbols: 30 °C. Full curves: recalculated with the parameters deduced from the best fit of experimental data.

CARBON-13 AND DEUTERIUM RELAXATION

Results. Carbon-13 experimental data concern only the carbons directly bound to a proton so that the dipolar contribution arises solely from the bound proton. Examination of the raw data showed that η/T_1 is independent of the measurement frequency and is also the same (within experimental uncertainties) for pure toluene and for toluene in the gel phase. This means that extreme narrowing conditions prevail for both samples,[16,17] this quantity, in that case, providing the proton−carbon dipolar cross-relaxation rate. Moreover, referring to eq 5, $R_1^{obs} = pR_1^{in} + (1-p)R_1^{out}$, the only way to explain the similarity of relaxation rates in pure liquid and in the gel phase is to assume $R_1^{dip,in} = R_1^{dip,out} = R_1^{dip,pure}$. As dipolar relaxation is here purely intramolecular (corresponding to the dipolar interaction of the considered carbon-13 with its bound proton), this means that molecular reorientation is essentially the same for "in" and "out" toluene. With reference to the considerations of the previous section, this means also that only translational motions are possibly affected when toluene is embedded in the organogel bundles. Now, it is well-known that, in extreme narrowing conditions, the dipolar contribution to the carbon-13 longitudinal relaxation rate is simply half the ratio η/T_1. Therefore, we have reported in Table 2 only the mean value (over the three measurement frequencies) of R_1^{dip}, while the contribution of other relaxation mechanisms (R_1^{others}) is deduced from $R_1^{obs} - R_1^{dip}$. Some deuterium relaxation measurements performed with toluene-d_5 (toluene labeled with deuterium on the aromatic

Table 3. Deuterium Spin−Lattice Relaxation Times (T_1, in s) of Toluene-d_5 (Labeling on the Aromatic Cycle) as Pure Liquid and in the Gel Phase[q]

	sample	
frequency (MHz)	pure toluene	gel phase
13.60	1.05 ± 0.05	1.03 ± 0.05
30.55	1.00 ± 0.05	n.m.
46.07	0.99 ± 0.05	0.97 ± 0.05
61.10	0.98 ± 0.05	0.96 ± 0.05

[q] Measurements were performed at 30°C at different frequencies.

Table 2. Separation of Carbon-13 Relaxation Rates (in s^{-1}) of Toluene into the Dipolar Contribution (Interaction with the Proton Directly Bound to the Considered Carbon) and the Contribution from Other Mechanisms

		20 °C			30 °C		
		C_2	C_3	C_4	C_2	C_3	C_4
pure toluene	R_1^{dip}	0.041 ± 0.003	0.042 ± 0.003	0.054 ± 0.004	0.037 ± 0.003	0.038 ± 0.003	0.048 ± 0.004
	R_1^{others} (75 MHz)	0.013 ± 0.005	0.014 ± 0.005	0.016 ± 0.006	0.012 ± 0.004	0.013 ± 0.004	0.014 ± 0.005
	R_1^{others} (100 MHz)	0.015 ± 0.005	0.016 ± 0.005	0.017 ± 0.006	0.015 ± 0.004	0.015 ± 0.004	0.016 ± 0.005
	R_1^{others} (150 MHz)	0.024 ± 0.005	0.025 ± 0.005	0.029 ± 0.006	0.022 ± 0.004	0.023 ± 0.004	0.026 ± 0.006
gel phase	R_1^{dip}	0.040 ± 0.003	0.040 ± 0.003	0.052 ± 0.004	0.035 ± 0.002	0.036 ± 0.002	0.047 ± 0.003
	R_1^{others} (75 MHz)	0.011 ± 0.004	0.011 ± 0.004	0.012 ± 0.006	0.011 ± 0.004	0.011 ± 0.004	0.013 ± 0.005
	R_1^{others} (100 MHz)	0.011 ± 0.004	0.013 ± 0.004	0.015 ± 0.006	0.012 ± 0.004	0.012 ± 0.004	0.014 ± 0.005
	R_1^{others} (150 MHz)	0.017 ± 0.005	0.019 ± 0.005	0.023 ± 0.006	0.016 ± 0.004	0.017 ± 0.004	0.020 ± 0.005

Table 4. Molecular Parameters Deduced from the Analysis of the Carbon-13 Relaxation Rates R_1^{dip} and R_1^{others}

		20 °C			30 °C		
		C_2	C_3	C_4	C_2	C_3	C_4
pure toluene	τ_c^{dip} (ps)	1.92 ± 0.13	1.94 ± 0.14	2.52 ± 0.18	1.72 ± 0.12	1.76 ± 0.12	2.25 ± 0.16
	R_1^{SR} (s^{-1})	0.009 ± 0.001	0.010 ± 0.001	0.010 ± 0.002	0.009 ± 0.001	0.010 ± 0.001	0.010 ± 0.002
	$\Delta\sigma^{pure}$ (ppm)	225 ± 16	227 ± 15	251 ± 18	225 ± 16	227 ± 15	251 ± 18
gel phase	τ_c^{dip} (ps)	1.86 ± 0.13	1.86 ± 0.13	2.44 ± 0.17	1.63 ± 0.11	1.66 ± 0.12	2.19 ± 0.15
	R_1^{SR} (s^{-1})	0.009 ± 0.001	0.008 ± 0.001	0.009 ± 0.002	0.009 ± 0.001	0.008 ± 0.001	0.009 ± 0.002
	$\Delta\sigma^{obs}$ (ppm)	166 ± 21	185 ± 18	210 ± 20	166 ± 21	185 ± 18	210 ± 20
upper limit	$\Delta\sigma^{out}$ (ppm)	215	237	269	215	237	269

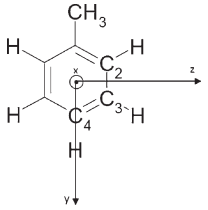

Figure 4. Definition of the *x*, *y* and *z* axes for the toluene molecule.

cycle, for a meaningful comparison with carbon-13 results) are reported in Table 3. As for carbon-13 dipolar relaxation, it is seen to be frequency independent and to be similar in pure liquid and in the gel phase. Because deuterium relaxation is governed exclusively by the quadrupolar mechanism, which is purely intramolecular, this confirms the above conclusions regarding the invariance of reorientational motions for pure toluene and for toluene in the gel phase.

Data Analysis. We start with the dipolar contribution which, under extreme narrowing conditions can be expressed as

$$R_1^{dip} = \left(\frac{\mu_0}{4\pi}\right)^2 \left(\frac{\gamma_H \gamma_C \hbar}{r_{CH}^3}\right)^2 \tau_c^{dip} \qquad (6)$$

where μ_0 is the vacuum permeability, γ's are gyromagnetic constants, r_{CH} is the length of the CH bond and τ_c^{dip} is an effective correlation time describing the reorientational motion of the CH bond. With r_{CH} = 1.09 Å, we obtain, for the three carbons C_2, C_3 and C_4, the effective correlation times given in Table 4. The fact that the effective correlation times are identical for C_2 and C_3 is a clear indication that the reorientation tensor is of axial symmetry, the symmetry axis being the *z* axis of Figure 4 (the axis *y* is the in-plane molecular symmetry axis while *x* is perpendicular to the aromatic cycle). This symmetry feature was first mentioned in the paper by Sturz and Dölle.[19] Moreover, in extreme narrowing conditions, the expression of effective correlation times can be easily derived from Woessner's theory.[22]

$$\tau_c^{eff} = \frac{9}{2}\sin^4\theta \frac{\tau_x\tau_z}{2\tau_x + 4\tau_z} + \frac{9}{2}\sin^2 2\theta \frac{\tau_x\tau_z}{\tau_x + 5\tau_z} + \frac{1}{4}(3\cos^2\theta - 1)^2\tau_x \qquad (7)$$

$\tau_x(=\tau_y)$ and τ_z describe the reorientation around the corresponding axis ,and θ is the angle between the CH bond and the reorientation tensor symmetry axis. From (C_2, C_3) and C_4 data we obtain, at 20 °C, τ_x = 1.8 ps and τ_z = 3.8 ps, and, at 30 °C, τ_x = 1.6 ps and τ_z = 3.3 ps, while, from the work of Sturz and Dölle,[19] one can derive the following values: τ_x = 1.7 ps and τ_z = 3.6 ps (at ambient temperature). Differences between pure toluene and toluene in the gel phase are within experimental error, confirming that rotational motions are merely the same for "out" toluene and "in" toluene.

Now, it can be noticed from Table 2 that, in all cases, R_1^{others} increases with the measurement frequency ν_{meas}. This is unambiguously indicative of a contribution of the so-called chemical shift anisotropy (csa) mechanism, the contribution of which can be written as

$$R_1^{csa} = \frac{2\tau_c^{csa}(2\pi)^2}{15}(\Delta\sigma)^2{\nu_{meas}}^2 \qquad (8)$$

where $\Delta\sigma$ stands for the csa (the shielding tensor being supposed of axial symmetry), and τ_c^{csa} stands for the correlation time describing the reorientation of the shielding tensor symmetry axis. Here, the shielding tensor symmetry axis is perpendicular to the aromatic cycle, and τ_c^{csa} is simply $\tau_c^{dip}(C_4)$. Thus, we can estimate the importance of the csa contribution at the three measurement frequencies (note that, if the shielding tensor is not exactly of axial symmetry, a factor equal to $(1 + \eta^2/3)$, with η being the so-called asymmetry parameter, has to be introduced in eq 8). As shown previously,[19] spin-rotation interaction is responsible for this third relaxation mechanism. The relevant contribution, denoted R_1^{SR}, will be assumed to be frequency independent. Experimental data have been fitted by assuming that η = 0, that $\Delta\sigma$(20 °C) = $\Delta\sigma$(30 °C), and that R_1^{SR}(30 °C) > R_1^{SR}(20 °C). Results of this procedure are reported in Table 4. There is not much to expect from R_1^{SR} because it represents roughly 15% of the total relaxation rate and is therefore prone to relatively large experimental uncertainties. Indeed, within these uncertainties, it does not exhibit significant variations regarding the sample. As already observed,[19] neither does it depend on temperature in the considered range.

Looking at $\Delta\sigma$ appears instructive since one observes a systematic decrease when going from pure toluene to toluene in the gel phase. As usual, this can be rationalized on the basis of eq 5 formulated here as $(\Delta\sigma^{obs})^2 = p(\Delta\sigma^{in})^2 + (1-p)(\Delta\sigma^{out})^2$. As the csa relaxation mechanism is purely intramolecular and acts exclusively through reorientational motions, which have been seen to be identical for both states ("in" and "out"), this decrease can only be attributed to modifications of the shielding tensor itself. Of course, the latter is very sensitive to minor changes of the electronic distribution at the level of each considered carbon. As $\Delta\sigma^{in}$ is unknown and even approximating $\Delta\sigma^{out}$ by $\Delta\sigma^{pure}$, we cannot hope to determine accurately *p* from the variation of $\Delta\sigma$ when going from pure liquid to the gel phase. Nevertheless,

Table 5. Self-Diffusion Coefficients of Pure Toluene (D^{pure}) and in the Gel Phase (D^{gel}) Together with the Self-Diffusion Coefficient in the Bound State (D^{in}) Calculated as Indicated in the Text

	20 °C	30 °C
D^{pure} (10^{-5} cm^2 s^{-1})	2.20 ± 0.07	2.40 ± 0.07
D^{gel} (10^{-5} cm^2 s^{-1})	1.85 ± 0.06	2.14 ± 0.06
D^{in} (10^{-5} cm^2 s^{-1})	1.3 ± 0.5	1.7 ± 0.6

as $p(\Delta\sigma^{in})^2$ is evidently positive, we can write $p \geq [(\Delta\sigma^{out})^2 - (\Delta\sigma^{obs})^2]/(\Delta\sigma^{out})^2$.This latter inequality can be formulated as follows:

$$p \geq 1 - \left(\frac{\Delta\sigma^{obs}}{\Delta\sigma^{out}}\right)^2 \quad (9)$$

With the p value determined in the previous section, we obtain from eq 9 $\Delta\sigma^{obs}/0.78$ as the upper limit for $\Delta\sigma^{out}$ (see Table 4). It turns out that this upper limit is consistently around $\Delta\sigma^{pure}$, the important point nevertheless being that $\Delta\sigma^{obs}$ is smaller than $\Delta\sigma^{pure}$. Thus, the part of the solvent embedded in the organogel is also revealed by carbon-13 relaxation, although the relevant mechanism is also intramolecular and therefore has the same reorientational features for "out" toluene and "in" toluene.

ANALYSIS OF TOLUENE SELF-DIFFUSION COEFFICIENTS AND OF THE LOW-FREQUENCY PART OF THE GEL PHASE ^{1}H DISPERSION CURVE

Self-diffusion coefficients of pure toluene and of toluene in the gel phase are given in Table 5 for the two temperatures considered here (20 and 30 °C); they are seen to evolve as expected with temperature. Self-diffusion coefficients are analyzed in the same way as relaxation rates (see eq 5)

$$D^{gel} = pD^{in} + (1-p)D^{out} \quad (10)$$

In order to calculate D^{in}, the value obtained for pure toluene (D^{pure} in Table 5) can been used (with some confidence) in place of D^{out}, whereas, as indicated above, p has been set to 0.4 (at both temperatures). It is reassuring to notice that the values found for D^{in} exhibit the expected variation with temperature. Moreover, the value of D^{in} is roughly two-thirds the value of D^{pure}, suggesting, in a speculative way, that diffusion within bundles is bidimensional rather than three-dimensional (isotropic) as in the pure liquid. However, these values of D^{in}, just a little smaller than those of pure toluene, indicate that the dynamics of toluene within the gel is not drastically modified. As rotational dynamics is not modified at all, it can be inferred that the first decay of the proton dispersion curve originates from intermolecular dipolar interactions which occur necessarily with the spins existing at the surface of fibers and not with the spins of other toluene molecules (since translational diffusion remains roughly that of pure liquid). On the other hand, the Lorentzian nature of this first decay, with a correlation time τ_c^{in} on the order of 10 μs, seems to be a good approximation, as confirmed by measurements of spin−lattice relation rates in the rotating frame by which the behavior at very low frequency (1 kHz to 5 kHz) can be probed.[23] As an alternative to a pertinent treatment of intermolecular dipolar relaxation, we can try to find out a physical meaning for the correlation time τ_c^{in}. It must be related to the diffusion coefficient, and, owing to the units of the latter, it is always possible to write

$$\tau_c^{in} = \frac{b_c^2}{D^{in}} \quad (11)$$

b_c would be a "correlation distance" and b_c^2 a sort of mean area over which toluene molecules travel for one second. Although somewhat tentative, this interpretation is model-free and leads to a plausible "correlation distance" ($b_c \approx 1000$ Å). A related approach was earlier proposed by Stapf et al.[24] but within an elaborated model. The correlation distance was shown to be similar to the pore size (∼50 Å). The much larger correlation distance found here could be related to the gel structure and to the fact that the solvent molecules can move along fibers of important length.

CONCLUSION

In this work, we were able to consistently analyze full proton dispersion curves of pure toluene and toluene in an organogel phase. Data of this first approach demonstrate that about 40% of toluene is embedded in the gel structure, so that we can state that the present system is of the "wet gel" type. The merit of this first approach is essentially to ascertain that part of toluene is actually in contact with the organogel and experiences some specific spin relaxation interactions. This does not mean that the solvent interacts with the gel and has something to do with its structure.

The second approach rests on the dipolar contribution to longitudinal relaxation of toluene carbons-13 directly bonded to protons. This contribution, being purely intramolecular, lends unambiguously to the conclusion that reorientational motions remain the same for pure toluene and toluene in the gel phase. This indicates clearly that toluene does not interact significantly with the gel and vice versa.

The third approach involves self-diffusion coefficients. It is observed that the self-diffusion coefficient of toluene embedded in the gel structure hardly drops (two-thirds of the one of pure toluene), this feature being explained by the lack of isotropy for translational motions. This result confirms that there exists no measurable interaction between gel and solvent.

It therefore emerges that the solvent does not play any significant role in the cohesion of the gel but rather fills free space within this structure. In other words, if the solvent is of prime importance in the gelation process, it becomes essentially passive once this process is completed. This explains, among other things, why such organogels can be relatively easily transformed into aerogels by solvent extraction.[25]

AUTHOR INFORMATION

Corresponding Author

*E-mail: Daniel.Canet@crm2.uhp-nancy.fr.

ACKNOWLEDGMENT

This work is part of the ANR project MULOWA (Grant Blan08-1_325450).

REFERENCES

(1) Terech, P.; Weiss, R. G. *Chem. Rev.* **1997**, *97*, 3133–3160.
(2) Weiss, R. G.; Terech, P. *Molecular Gels*; Springer: Dordrecht, Netherlands, 2006.

(3) Terech, P.; Pasquier, D.; Bordas, V.; Rossat, C. *Langmuir* **2000**, *16*, 4485–4494.
(4) George, M.; Weiss, R. G. *Chem. Mater.* **2003**, *15*, 2879–2888.
(5) Moniruzzaman, M.; Sundararajan, P. R. *Langmuir* **2005**, *21*, 3802–3807.
(6) Huang, X.; Terech, P.; Raghavan, S. R.; Weiss, R. G. *J. Am. Chem. Soc.* **2005**, *127*, 4336–4344.
(7) Schmidt, R.; Adam, F. B.; Michel, M.; Schmutz, M.; Decher, G.; Mésini, P. J. *Tetrahedron Lett.* **2003**, *44*, 3171–3174.
(8) Suzuki, M.; Nigawara, T.; Yumoto, M.; Kimura, M.; Shirai, H.; Hanabusa, K. *Tetrahedron Lett.* **2003**, *44*, 6841–6843.
(9) Brosse, N.; Barth, D.; Jamart-Grégoire, B. *Tetrahedron Lett.* **2004**, *45*, 9521–9524.
(10) Pham, Q. N.; Brosse, N.; Dumas, D.; Hocquet, A.; Jamart-Grégoire, B. *New J. Chem.* **2008**, *32*, 1131–1139.
(11) Hamada, D.; Yanagihara, I.; Tsumoto, K. *Trends Biotechnol.* **2004**, *22*, 93–97.
(12) Jeong, Y.; Hanabusa, K.; Masunaga, H.; Akiba, I.; Miyoshi, K.; Sakurai, S.; Sakurai, K. *Langmuir* **2005**, *21*, 586–594.
(13) Kimmich, R. *NMR: Tomography, Diffusometry, Relaxometry*; Springer: Berlin, 1997.
(14) Aroulanda, C.; Starovoytova, L.; Canet, D. *J. Phys. Chem. A* **2007**, *111*, 10615–10624.
(15) Teng, C.-L.; Hong, H.; Kiihne, S.; Bryant, R. G. *J. Magn. Reson.* **2001**, *148*, 31–34.
(16) Kowaleski, J.; Mäler, L. *Nuclear Spin Relaxation in Liquids: Theory, Experiments and Applications*; Taylor & Francis: New York, 2006.
(17) Canet, D. *Nuclear Magnetic Resonance: Concepts and Methods*; Wiley: Chichester, U.K., 1996.
(18) Belorizky, E.; Fries, P. H.; Helm, L.; Kowalewski, J.; Kruk, D.; Sharp, R. R.; Westlund, P.-O. *J. Chem. Phys.* **2008**, 052315.
(19) Sturz, L.; Dölle, A. *J. Phys. Chem. A* **2001**, *105*, 5055–5060and references therein.
(20) Nordstierna, L.; Yushmanov, P. V.; Furó, I. *J. Chem. Phys.* **2006**, *125*, 074704.
(21) Belorizky, E.; Fries, P.; Guillermo, A.; Poncelet, O. *ChemPhysChem* **2010**, *11*, 2021–2026.
(22) Woessner, D. E. *J. Chem. Phys.* **1962**, *37*, 647–654.
(23) Steiner, E.; Yemloul, M.; Guendouz, L.; Leclerc, S.; Robert, A.; Canet, D. *Chem. Phys. Lett.* **2010**, *495*, 287–291.
(24) Stapf, S.; Kimmich, R.; Seitter, R.-O. *Phys. Rev. Lett.* **1995**, *75*, 2855–2858.
(25) Brosse, N.; Barth, D.; Jamart-Grégoire, B. *Tetrahedron Lett.* **2004**, *45*, 9521–9524.